Modeling and Control of Voltage Source Converters Interfacing Renewable Energy Sources in Weak Grid Conditions

Daichi Tamai, Owen Massey, Issam Khouri, and Amr Radwan

Abstract: This work presents a robust current control strategy of the grid-connected voltage source converter (VSC) via the mixed-sensitivity design approach. The objective is to maintain a well-damped performance under a wide variation range of the utility-grid impedance. The plant is modelled and controlled in the stationary reference frame. Firstly, the performance weighting function is designed to ensure a good current tracking at the line frequency. Secondly, the robustness weighting function is designed by considering the worst case of the multiplicative output unstructured uncertainty in the utility-grid impedance. A constant weighting function is considered to penalize the controller effort. Finally, the $H\infty$ robust controller is synthesised to minimize the infinity norm of the cost function that combines the weighted sensitivity, complementary sensitivity, and the function from the reference to the controller output. Time-domain simulations are presented and compared to similar scenarios with the proportional-and-integral and proportional-resonant current controllers.

I. Introduction

Distributed generation (DG) systems have been widely adopted to compensate the environmental, technical, and economical challenges of the conventional fuel-fired power generation. In grid-connected applications, the three-phase voltage source converters (VSCs) play the key role to interface the renewable energy resources. The current control strategies can be achieved either in the rotating reference frame via the proportional-and-integral (PI) controllers or in the stationary reference frame via the proportional-resonant (PR) controllers [1]-[2]. The former transforms the sinusoidal quantities into time-invariant components and hence an easier tracking can be achieved by the integral gain. However, a phase-locked-loop (PLL) is required to align the rotating two-phase components to the point-of-common coupling (PCC) voltage. The later controller is promising as it achieves a zero-tracking error for the sinusoidal references while no PLL is needed for orientation. However, both controllers are designed for the nominal plant to guarantee the nominal performance and stability. It is shown in this work that the variations in the utility-grid impedance negatively affect the performance of the PI and PR controllers. Therefore, a robust $H\infty$ controller is synthesised to control the injected currents under a wide variation range of the utility-grid impedance [3]-[5]. The robust controller synthesis is achieved by minimizing the infinity norm of the cost function that combines the weighted sensitivity, complementary sensitivity and the controller effort functions. The problem is solved by the mixed-sensitivity approach in the Matlab robust control toolbox [5]-[6]. Time-domain simulations evaluate the performance of the robust, the PI, and PR controlled grid-connected VSC.

II. Mixed-Sensitivity $H\infty$ Robust Control – Background

Fig. 1 shows the system under study where a three-phase VSC is connected to the utility-grid via an inductive filter (L) with an internal resistance R; v_t, v, v_g are the three-phase terminal voltage of the VSC, the PCC voltage, and the utility-grid voltage, respectively; L_g, R_g are the equivalent grid inductance and resistance, respectively. In this work, the proposed robust current controller is compared to the PI and the PR current controllers.

A block diagram of the standard one-degree-of-freedom feedback control system is shown in Fig. 2(a) where r, y, e, u, and d are the reference, plant output, the tracking error, control signal, and disturbance input, respectively; $G_n(s)$ represents the model of the nominal plant to be controlled whereas $K(s)$ is the fixed controller to be designed. Out of this block diagram, the following relations are yielded

$$L(s) = G_n(s)K(s),$$
$$S(s) = \frac{e}{r} = \frac{y}{d} = \frac{1}{1+L(s)},$$
$$T(s) = \frac{y}{r} = \frac{L(s)}{1+L(s)} \quad (1)$$

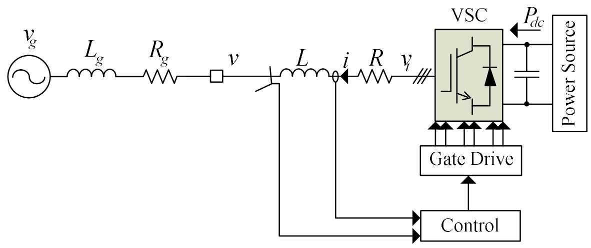

Fig. 1. Grid-connected VSC

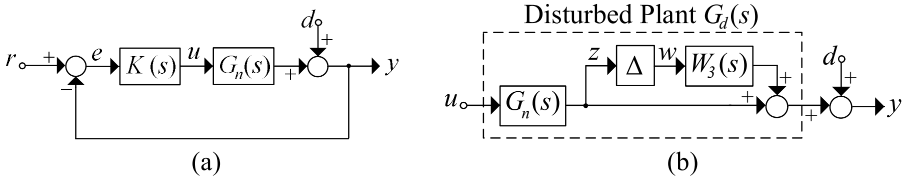

Fig. 2. Block diagram of one-degree-of-freedom feedback control system. (a) Standard setup. (b) Multiplicative unstructured uncertainties.

where $L(s)$ is the loop gain; $S(s)$ and $T(s)$ are the sensitivity and complementary sensitivity functions. It is noted that $S(s)$ should be minimized to achieve a good tracking performance and disturbance rejection. Moreover, $T(s)$ should be minimized to maintain the closed loop stability. However, $S(s) + T(s) = 1$ and hence they cannot be minimized simultaneously. Therefore, frequency dependent weighting functions, referred to as $W_1(s)$ and $W_3(s)$, are used to minimize $S(s)$ and $T(s)$ in separated frequency regions, i.e. $min|W_1(j\omega)S(j\omega)|$ and $min|W_3(j\omega)T(j\omega)|$, such that the summation of the weighted sensitivity and complementary sensitivity functions is unity for any frequency. Typically, the sensitivity function is minimized in the low frequency region whereas the complementary sensitivity function is minimized at high frequencies. Referring to Fig. 2(b),

$$G_d(s) = G_n(s)(1 + W_3(s)\Delta(s)),\\ \|\Delta(j\omega)\|_\infty \leq 1, \forall\omega \tag{2}$$

where $\Delta(s)$ is a stable transfer function bounded by unity at any frequency; $G_d(s)$ and $G_n(s)$ are the transfer functions of the disturbed and nominal plant, respectively.

The preceding discussion is formally referred to as the *mixed-sensitivity* robust control design and the corresponding generalized setup is shown in Fig. 3 where $K(s)$ is the $H\infty$ controller. An additional weighting function, $W_2(s)$, is added to the setup to penalize the controller effort. The $H\infty$ optimal controller is synthesised following (3).

$$\|T_{zw}(j\omega)\|_\infty = \left\| \begin{matrix} W_1(j\omega)S(j\omega) \\ W_2(j\omega)K(j\omega)S(j\omega) \\ W_3(j\omega)T(j\omega) \end{matrix} \right\|_\infty < 1, \forall\omega \tag{3}$$

where T_{zw} is the equivalent transfer function from w to z in Fig. 3.

III. Mixed-Sensitivity $H\infty$ Robust Control – Design Procedures

In this section, the $H\infty$ robust control is designed for the grid-connected VSC to account for the influence of the utility-grid parameters variations.

A. Weighting Function for Tracking Performance – $W_1(s)$

This weighting function shapes the sensitivity function such that $\|S(j\omega)\|_\infty \leq W_1^{-1}(j\omega)$ where $S(j\omega)$ is the transfer function between the error and reference. This implies that $S(j\omega)$ should be small at the neighbourhood of the line frequency to track the sinusoidal reference currents in the stationary reference frame. In other words, $W_1^{-1}(j\omega)$ should reflect a high gain around 60 Hz while providing a small gain elsewhere. Therefore, $W_1(s)$ is selected as shown in (4).

$$W_1(s) = \frac{k\omega_\circ}{s^2+2\xi\omega_\circ s+\omega_\circ^2} \tag{4}$$

where $\omega_\circ$ is the line frequency in rad/sec, ξ is the damping ratio whereas k is a gain to adjust the tracking error.

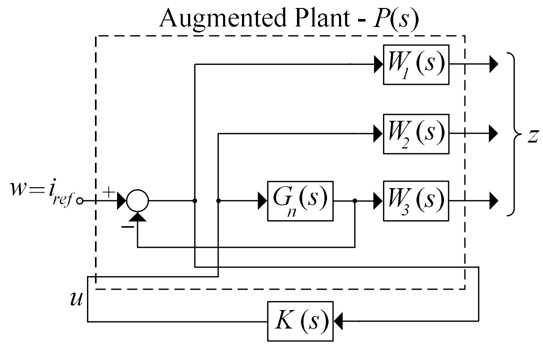

Fig. 3. Standard $H\infty$ control configuration via the mixed-sensitivity approach.

B. Weighting Function for Control Effort – W_2

This weighting is a small constant to penalize the control effort. In this work, $W_2 = 0.05$.

C. Weighting Function for Robust Performance – $W_3(s)$

This weighting function shapes the complementary sensitivity function such that $\|T(j\omega)\|_\infty \leq W_3^{-1}(j\omega)$ where $T(s)$ represents the closed loop transfer function from the reference input to the output. Further, it is responsible for the closed loop tracking and hence it should be close to unity in the low frequency region.

$$W_3(s)\Delta(s) = \left(\frac{G_d(s)-G_n(s)}{G_n(s)}\right) \tag{5}$$

From (5) and as $\|\Delta(j\omega)\|_\infty \leq 1$, $\forall\omega$, $W_3(s)$ should be designed by considering the worst-case uncertainty spectrum to account for the worst deviation from the nominal conditions. Therefore, (6) is yielded.

$$W_3(s) \geq \bar{\sigma}\left(\frac{G_d(s)-G_n(s)}{G_n(s)}\right) \tag{6}$$

Following (6), the weighting function can be selected as shown in Fig. 4(a) where it has a large gain at high frequencies and small gain at low frequencies. Following the 0-dB coordination criterion, $W_3(s)$ is selected as shown in (7) and Fig. 4(b).

$$W_3(s) = \frac{0.0002s+0.803}{0.0001s+1} \tag{7}$$

D. Mixed-Sensitivity H∞ Robust Control Synthesis

The mixed-sensitivity robust controller can be synthesised using the Matlab Robust Control Toolbox [5]. The controller is shown in (8) whereas a reduced third order controller is shown in (9).

$$K(s) = \frac{(7.944e5)s^3+(8.037\quad)s^2+(9.32\qquad)s+1.545}{s^4+7.429e4\ \ ^3+1.031e9s^2+(1.6e1\ \ )s+1.465e} \tag{8}$$

$$K(s) = \frac{(8.086e5)s^2+(5.634\quad)s+3.829e}{s^3+(7.049\quad)s^2+(5.117e5)s+1.001e10} \tag{9}$$

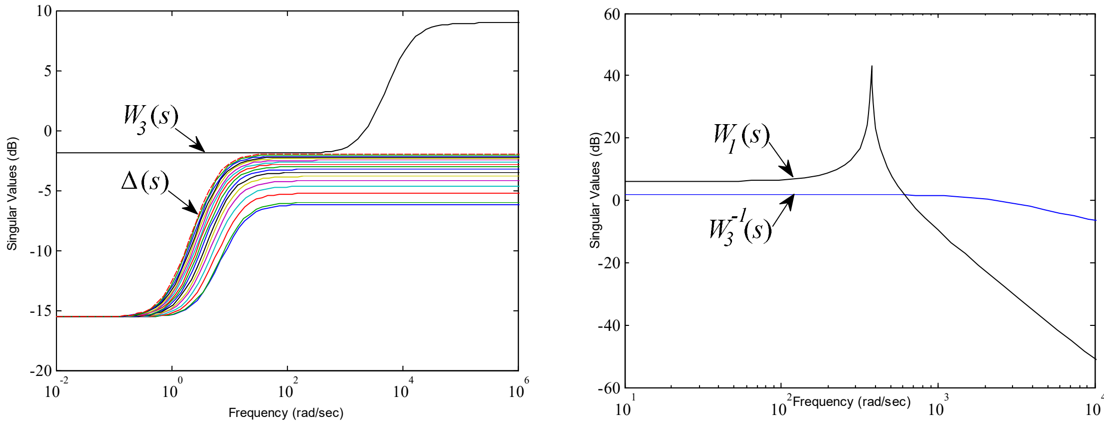

(a) (b)

Fig. 4. Weighting functions design. (a) $W_3(s)$. (b) 0-dB criterion.

The performance of the fourth and third order controllers are analysed as shown in Fig. 5. In both cases, the sensitivity function is less than $W_1^{-1}(s)$ whereas the complementary sensitivity function is less than $W_3^{-1}(s)$, for all frequencies. The sensitivity function has a very low gain at the line frequency to achieve the sinusoidal current tracking.

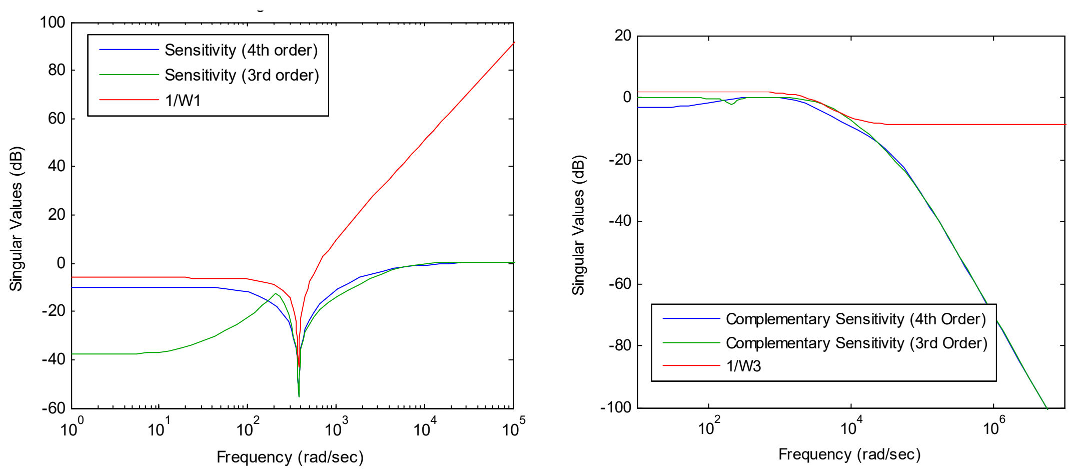

(a) (b)

Fig. 5. Singular values. (a) Sensitivity function. (b) Complementary sensitivity function.

I. Evaluation Results

The influence of the grid impedance on the dynamics of the grid connected VSC is shown in Fig. 6. The VSC is interfaced by a $2.4mH$ to the PCC. As shown in Figs. 6(a)-(b), the dc and ac voltage are lightly damped due to the high interfacing impedance. Note that the vector control scheme of the VSC and the PWM generation are implemented on the dSPACE1104 control card supported with a TMS320F240-DSP coprocessor structure for PWM generation. The software code is generated by the Real-Time-WorkShop under a Matlab/Simulink environment.

For further investigations, a time-domain Matlab/Simulink model for the system in Fig. 1 has been built to evaluate the performance of the designed robust controller. For the sake of comparison, the similar model has been tested with a first order PI and a second order PR current controllers. Both controllers have been designed for the nominal parameters of the VSC and the utility-grid. In the time-domain model, the utility-grid impedance is set to the nominal value at $2.3\ mH$. At $t = 0.5\ s$, the grid-impedance increases to $10\ mH$. The performance of the system following the utility-grid parameters variation is shown in Fig. 7 where the robust controlled system reflects the highest damping performance. On the contrary, the PI and PR controlled systems are lightly damped against the utility-grid parameters variations.

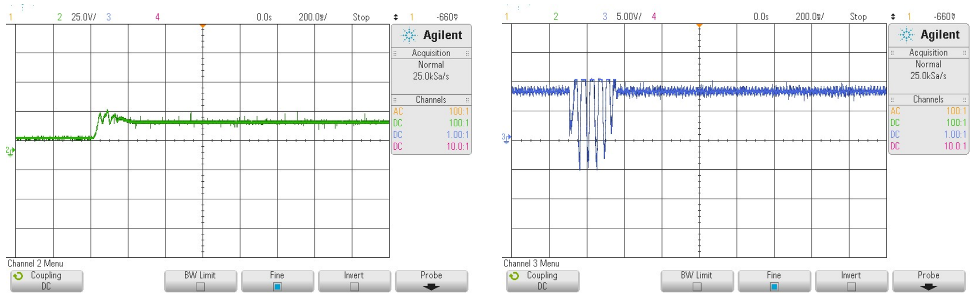

(a) (b)

Fig. 6. Vector control of VSC in the rectification mode – starting on a high grid impedance. (a) DC voltage. (b) d-component of the ac voltage.

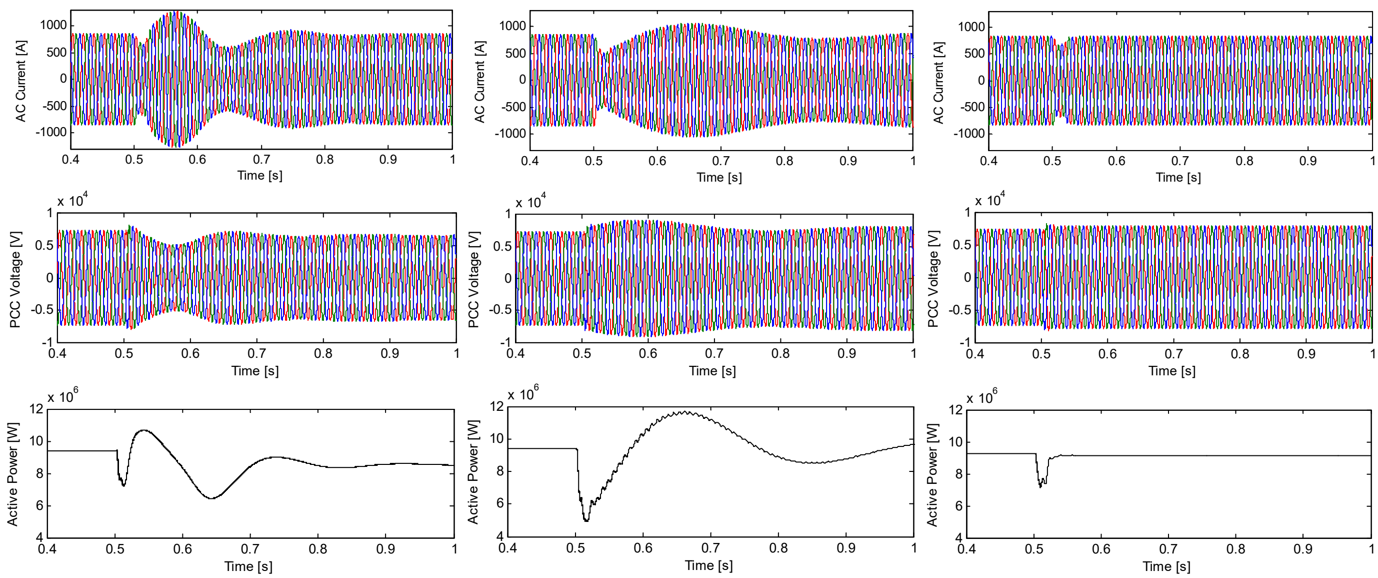

(a) (b) (c)

Fig. 7. Time-domain simulation results. (a) PI current control. (b) PR current control. (c) Robust control.

II. Conclusion

A mixed-sensitivity $H\infty$ robust controller has been designed for the grid-connected VSC under a wide variation range of the utility-grid impedance. The design depends on the proper selection of the weighting functions to achieve a robust performance and stability. Time-domain simulations show that the robust control provides the highest damping performance as compared to the PI and the PR controlled system.

References

[1] Yazdani, A., and Iravani, R.: '*Voltage-sourced converters in power systems: Modeling, control, and applications*' New Jersey: John Wiley & Sons, 2010.

[2] D. N. Zmood and D. G. Holmes, "Stationary frame current regulation of PWM inverters with zero steady-state error," *IEEE Trans. Power Electron.*, vol. 18, no. 3, pp. 814–822, May 2003.

[3] S. Yang, Q. Lei, F. Peng, and Z. Qian, "A robust control scheme for grid-connected voltage-source inverters," *IEEE Trans. Ind. Electron.*, vol. 58, no. 1, pp. 202-212, 2011.

[4] Y. Li, D. Vilathgamuwa, F. Blaabjerg, and P. Loh, "A robust control scheme for medium-voltage-level DVR implementation," *IEEE Trans. Ind. Electron.*, vol. 54, no. 4, pp. 2249-261, 2007.

[5] Math Work Inc., "Robust Control Toolbox User's Guide," Mar. 2000.

[6] A. Radwan, X. Jiang, D. Tamai, O. Massey, and I. Khouri, "Performance evaluation of grid-connected converters using the mixed sensitivity robust current control," in Proceedings of the Mediterranean Conference on Control and Automation, pp. 398-402, 2021